

## **IEEE copyright notice**

Personal use of this material is permitted. However, permission to reprint/republish this material for advertising or promotional purposes or for creating new collective works for resale or redistribution to servers or lists, or to reuse any copyrighted component of this work in other works must be obtained from the IEEE. Contact: Manager, Copyrights and Permissions / IEEE Service Center / 445 Hoes Lane / P.O. Box 1331 / Piscataway, NJ 08855-1331, USA. Telephone: + Intl. 908-562-3966.

# Extending the Frequency Matching in Linear FMCW Radar Exploiting Extreme Frequencies

Marcus Reiher and Bin Yang

Chair of System Theory and Signal Processing, Universität Stuttgart

Pfaffenwaldring 47, 70550, Stuttgart, Germany

email: {marcus.reiher, bin.yang}@Lss.uni-stuttgart.de

**Abstract**—Frequency matching is an essential block of the signal processing chain in LFM CW (linear frequency modulated continuous wave) radar. Its task is to associate frequency detections obtained in multiple measurements. Under certain conditions, this association may fail and frequency detections from multiple real targets may be combined to a mismatch. The classification of a frequency association as match (real target) or mismatch (ghost target) is commonly regarded impossible if we only have frequency detections. Yet in this paper we show that even in this case, a reliable classification is possible when special attention is paid to the two outermost frequencies in each spectrum. Furthermore, the radar’s modulation can be designed such that the reliable classification can be achieved in the regions of interest of the distance-velocity-plane, i.e. application-specific.

**Index Terms**—chirp radar, FMCW, extreme frequency, waveform design

## I. INTRODUCTION

Frequency matching is an essential block of the signal processing chain in LFM CW radar. Its task is to associate frequency detections obtained in multiple measurements. Under certain conditions, this association may fail and frequency detections from multiple real targets may be combined to a ghost target, referred to as a mismatch. But most applications employing an LFM CW radar are required to be robust with respect to ghost targets and hence should be able to recognize them. Especially in the field of automotive radar, there is an ongoing extension of radar applications from driver assistance systems, e.g. ACC (adaptive cruise control), to safety systems. The major task of such systems is the early detection of dangerous situations and an appropriate counter measure like emergency break. Clearly, those systems do have an increasing demand for highly reliable sensor decisions and thus the avoidance of mismatches plays a major role in the design of an LFM CW radar system.

The classification of a frequency association as match (real target) or mismatch (ghost target) is commonly regarded impossible if we only have frequency detections. Without additional information, e.g. amplitudes, phases, or direction of arrival, a distinction between a match and a mismatch is impossible. Yet in this paper we show that even in this case, a reliable classification is possible for some matches when special attention is paid to the two outermost frequencies in each spectrum. These frequencies are called extreme frequencies below. Furthermore, the radar’s modulation can be designed such that the reliable classification can be achieved in the regions of interest of the distance-velocity-plane, i.e. according to the application. With the term modulation, we refer to a sequence of  $N$  frequency ramps. Each ramp is a linear up- or downsweep of the radar’s transmit frequency as a function of time.

The outline of this paper is as follows: In section II, we briefly review the basic properties and equations of the LFM CW radar. In section III, we introduce the concept of extreme matches or

simply eMatches, prove its existence under certain conditions, discuss its properties, and present two improved frequency matching algorithms by utilizing eMatches. In section IV, simple design rules for a modulation for ACC application are drawn. Simulation results are given in section V. Conclusions are drawn in section VI.

## II. LFM CW MODULATION

### A. The LFM CW equation

The basics of LFM CW will not be derived here, as there are various introductory works about this topic like [1]. We start by presenting the so called LFM CW equation which links the target parameters to be estimated, distance  $d$ [m] and relative radial velocity (negative for closing targets)  $v$ [ $\frac{m}{s}$ ], to the beat frequency  $f$ [Hz], defined as the difference between the transmitted and received frequency. In LFM CW, the radar’s transmit frequency is swept linearly as a function of time, with a slope of  $s$ [ $\frac{Hz}{s}$ ] and centered at the carrier frequency  $f_c$ [Hz]. We call such an up- or downsweep a frequency ramp, or simply a ramp. The resulting beat frequency  $f$  is given by

$$f = \frac{2}{c} (sd + f_c v) = \underbrace{\frac{2}{c} [s \quad f_c]}_{\underline{a}^T} \underbrace{\begin{bmatrix} d \\ v \end{bmatrix}}_{\underline{p}} = \underline{a}^T \underline{p}, \quad (1)$$

where  $c$  is the speed of light. Equation (1) corresponds to a straight line in the  $(dv)$ -plane

$$v = -\frac{s}{f_c} d + \frac{cf}{2f_c}, \quad (2)$$

a so called  $(dv)$ -line. For an up- (positive slope) or downsweep (negative slope) of the transmit frequency, the  $(dv)$ -line decays or rises linearly. To determine the target parameters  $(d, v)$ , a second ramp with a different slope is necessary. The target is then determined at the intersection of both  $(dv)$ -lines. In general, when we use  $N$  ramps to measure  $M$  targets, equation (1) can be extended to

$$\mathbf{F} = \begin{bmatrix} f_{11} & \dots & f_{1M} \\ \vdots & \ddots & \vdots \\ f_{N1} & \dots & f_{NM} \end{bmatrix} \stackrel{(1)}{=} \underbrace{\begin{bmatrix} \underline{a}_1^T \\ \vdots \\ \underline{a}_N^T \end{bmatrix}}_{\mathbf{A}} \underbrace{\begin{bmatrix} p_1, \dots, p_M \end{bmatrix}}_{\mathbf{P}} = \mathbf{A}\mathbf{P}, \quad (3)$$

where the  $i$ -th row of the  $N \times M$  frequency matrix  $\mathbf{F}$  contains  $M$  beat frequencies  $f_{ij}$  caused by a particular ramp  $\underline{a}_i$  and targets  $p_j$ . Targets are then determined as intersections of all  $N$   $(dv)$ -lines of different slopes. In the radar literature, the procedure to determine the target parameters  $\mathbf{P}$  from the modulation  $\mathbf{A}$  and the frequency measurements  $\mathbf{F}$  is referred to as *frequency matching*.

### B. Frequency matching as an assignment problem

No matter how many ramps are used in a modulation, it is always possible to construct a pattern of  $M(\geq N)$  targets causing more than  $M$  intersections of  $N$  ( $dv$ )-lines. The consequence is the occurrence of mismatches, refer to Fig. 1. This means,  $N$  ramps are not always enough to determine  $M(\geq N)$  targets uniquely, but there will be no mismatches if  $M < N$ . As measurement noise is always present, approximate intersections have to be accounted for, too. This further complicates the classification of matches. The mathematical foundations of the assignment problem can be found in [2], a brief introduction to frequency matching for FMCW radar is given in [3].

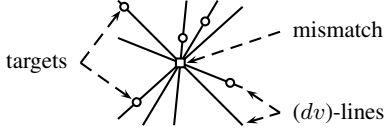


Fig. 1. A mismatch for  $M$  targets and  $N$  ramps ( $M \geq N$ ), here  $N = M = 5$

Usually, the frequency matching algorithm only knows the modulation parameters  $\underline{a}_i$  and the detected beat frequencies  $f_{ij}$  in (3). For each beat frequency  $f_{ij}$ , a ( $dv$ )-line of the frequency ramp  $\underline{a}_i$  can be drawn in the ( $dv$ )-plane on which the  $j$ -th real target must be located. In total, with the frequency matrix  $\mathbf{F}$  in (3) we can draw  $N$  groups of parallel ( $dv$ )-lines corresponding to the  $N$  different frequency ramps. If  $M \geq N$ , there may be more than  $M$  intersections of  $N$  ( $dv$ )-lines. Among them,  $M$  intersections correspond to the real targets and the remaining ones are mismatches. This is illustrated in Fig. 2. In the top row,  $N = 4$  frequency ramps of a modulation are depicted. The second row shows the respective idealized spectra when  $M = 3$  targets are present, which are labeled according to their numbering in the ( $dv$ )-plane shown below. Seven intersections of ( $dv$ )-lines from the first three ramps do occur. The three of them marked as white circles correspond to the real targets  $T_1$ ,  $T_2$  and  $T_3$ ; the four gray squares represent mismatches. Without additional information provided by the fourth ramp, a further classification of these seven intersections as matches or mismatches seems to be impossible. In this paper we will show that a reliable classification of these matches is possible under certain conditions.

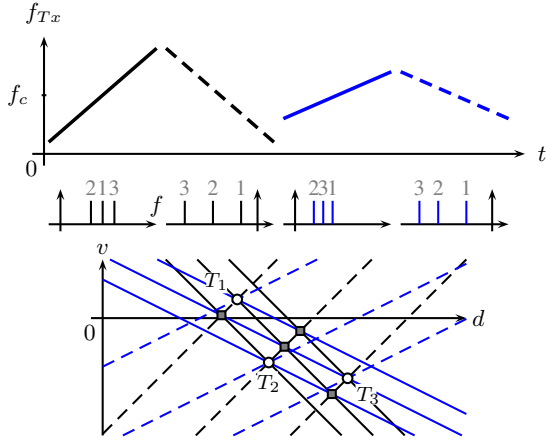


Fig. 2. Impossible classification for  $N = 3$  ramps sensing  $M = 3$  targets. This becomes possible if we use  $N = 4$  ramps.

### III. EXTREME MATCHES

In this section, we introduce the concept of extreme matches and study their basic properties. The standard frequency matching consists of two steps:

- S1) From the modulation parameters in  $\mathbf{A}$  and the frequency matrix  $\mathbf{F}$  in (3), estimate the number  $M$  of targets present. This task is known as order estimation.
- S2) From  $\mathbf{A}$  and  $\mathbf{F}$ , estimate the positions  $\mathbf{P}$  of all targets in the ( $dv$ )-plane. This task is known as parameter estimation.

Below we introduce an additional step in frequency matching:

- S3) From  $\mathbf{A}$  and  $\mathbf{F}$ , determine the so called extreme matches caused by at least three extreme frequencies.

#### A. Extreme frequency and extreme match

Without loss of generality, we limit our focus to the case where  $M > 1$  targets are present. If  $M \leq 1$ , no mismatches could occur if we use  $N \geq 2$  ramps. We consider two special frequencies in each spectrum  $i$

$$f_{i,\min} := \min_j(f_{ij}), \quad (4)$$

$$f_{i,\max} := \max_j(f_{ij}) \quad (5)$$

and refer to them as *extreme frequencies*. They are the left-most and right-most beat frequencies in the spectrum of frequency ramp  $i$ . In general, we will have  $f_{i,\min} < f_{i,\max} \forall i$ , although it might happen that all frequencies coincide in one spectrum, i.e.  $f_{i,\min} = f_{i,\max}$ . If this is the case in spectrum  $i_0$ , we will definitely have  $f_{i,\min} < f_{i,\max}$  in all other spectra  $i \neq i_0$  because otherwise only one target is present which contradicts our assumption  $M > 1$ .

For each extreme frequency, the corresponding ( $dv$ )-line is called an *extreme (dv)-line*. It is important to note that all ( $dv$ )-lines and hence all targets are located somewhere between the respective extreme ( $dv$ )-lines for each frequency ramp. This is shown in Fig. 3. Now it may happen that among the matches found by the frequency matching algorithm, some of them are caused by  $e \geq 3$  extreme frequencies. In the following, we refer to such matches as *extreme matches* or simply *eMatches*.

#### B. Existence

Inspired by a proof given in [4], we show in the following that the existence of an extreme match is assured when we have less targets than ramps, i.e.  $M < N$ . First we make the following ideal assumptions.

- A1) The modulation  $\mathbf{A}$  has  $N \geq 3$  ramps.
- A2)  $M$  targets are present with  $1 < M < N$ .
- A3) The probability of spectral detection is  $P_D = 1$ .
- A4) The probability of spectral false alarm is  $P_{FA} = 0$ .
- A5) No quantization in frequency or other measurement errors.

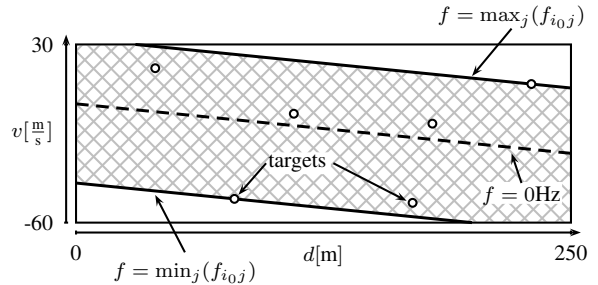


Fig. 3. Two extreme ( $dv$ )-lines in spectrum  $i_0$  and  $M = 6$  targets

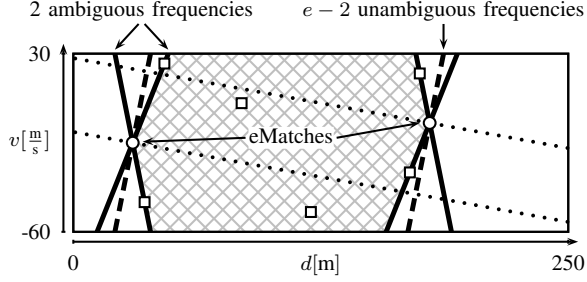


Fig. 4.  $(dv)$ -plane with two extreme matches for  $N = 4$  ramps

A6) The radar is equipped with an IQ-mixer.  
Starting with these assumptions, we conclude:

- In (almost) every spectrum there will be two extreme frequencies. If there is one spectrum with just one extreme frequency (all frequencies coincide), all other spectra will have two extreme frequencies. Thus in total we have  $2N - 1$  extreme frequencies at least.
- A partition of the  $2N - 1$  extreme frequencies to  $M$  targets ( $M < N$ ) such that every target consists of at maximum two extreme frequencies is impossible due to  $2M \leq 2(N - 1) < 2N - 1$ . Hence there is at least one target with at least three extreme frequencies. So for  $M < N$  we always have at least one extreme match.
- For  $M \geq N$ , extreme matches are not assured to exist, but they can exist for arbitrary  $M$ . Fortunately, the design of modulation has a strong influence on the occurrence of extreme matches.

### C. Properties

Matches found as extreme matches have a very appealing property: They are always real targets and *never* mismatches. In Fig. 4, a part of the  $(dv)$ -plane is depicted with two targets shown as white circles together with their respective  $(dv)$ -lines for a 4-ramp modulation. Some additional targets are shown as white squares. Furthermore, a hatched area analog to Fig. 3 is depicted, now constrained by three pairs of extreme  $(dv)$ -lines which are plotted bold. Per definition, at the position of an extreme match,  $e \geq 3$  extreme  $(dv)$ -lines do intersect. In the example in Fig. 4, we have two extreme matches (white circles) with  $e = 3$ . In analogy to Fig. 3, all targets must be located in the hatched area or on its boundary. The two extreme frequencies bounding the hatched area may be ambiguous, i.e. there may be multiple targets causing the same beat frequency in the respective ramp. This situation is depicted in Fig. 4. The remaining  $e - 2$  extreme frequencies of each extreme match, however, are unambiguous. In general, at the position of an extreme match with  $e$  extreme frequencies, the  $(dv)$ -plane is divided into  $2e$  regions. All targets are located inside just one of these regions or on its boundary. Yet this region is bounded by only two of the extreme  $(dv)$ -lines (solid bold lines in Fig. 4). Hence  $e - 2 > 0$  extreme  $(dv)$ -lines (dashed bold line in Fig. 4) have only one single point in common with the hatched area, the position of the extreme match itself. Under the assumption of ideal spectral detection properties, i.e. probability of detection  $P_D = 1$  and probability of false alarm  $P_{FA} = 0$ , the presence of the  $e - 2$  remaining extreme  $(dv)$ -lines guarantees that the extreme match corresponds to a real target and never to a mismatch. This fact is not changed by the remaining  $N - e$  frequencies and the corresponding non-extreme  $(dv)$ -lines (dotted line in Fig. 4).

Note that a later step in the signal processing chain of a

FMCW radar could be the estimation of the direction of arrival (DOA) for each match found. This estimation is very sensitive to frequency overlap, i.e. when the beat frequencies caused by multiple targets are very close to each other in the spectrum of a certain ramp, refer to [5] for further details. Since we have shown that every extreme match consists of  $e - 2$  unambiguous extreme frequencies, it is beneficial to use these frequencies for DOA estimation.

### D. Passive and active eMatching

Basically, there are two ways to exploit the properties of extreme matches to improve the frequency matching. One is to perform the standard frequency matching and scan its output for eMatches at the end. This method is simple and we will refer to it as *passive eMatching*. The other one is slightly complicated since it integrates the detection of eMatches into the process of standard frequency matching. Thus it is named *active eMatching*. It works iteratively and tries to first match the extreme frequencies only. If an eMatch is found, its  $e - 2$  unambiguous extreme frequencies are removed and the process is repeated again with a new set of extreme frequencies.

Below we discuss the passive and active eMatching in detail. The algorithm for passive eMatching can be summarized as follows:

- 1) Perform the standard frequency matching.
- 2) Label frequencies of all matches as extreme or not.
- 3) Search all matches for such consisting of more than two extreme frequencies. They are eMatches.
- 4) Identify the  $e - 2$  unambiguous frequencies in each eMatch and mark them for later use in DOA estimation.

Fig. 5 illustrates the execution of the algorithm. As similar to Fig. 4, a  $(dv)$ -plane with targets marked as white circles and squares is depicted. The extreme  $(dv)$ -lines of this particular target pattern are plotted bold for a four ramp modulation. In step 2 and 3, the matches marked by white circles will be identified as eMatches. Their unambiguous frequencies (dashed lines) are labeled in step 4.

The algorithm has a low additional computational complexity. Yet its benefit is moderate as there is no intervention to the standard frequency matching. The stability of the algorithm is assured because the set of matches found remains unchanged compared to the standard frequency matching.

The algorithm for active eMatching can be summarized as follows:

- 1) Perform iteratively until all eMatches have been processed:
  - a) Standard frequency matching using *extreme frequencies only*.
  - b) Identify eMatches, label  $e - 2$  unambiguous frequencies in each eMatch.
  - c) Remove *unambiguous* extreme frequencies.

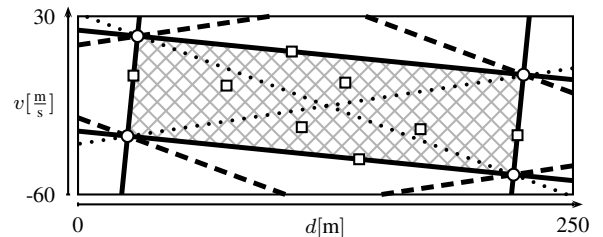


Fig. 5. Passive eMatching and iteration one of active eMatching

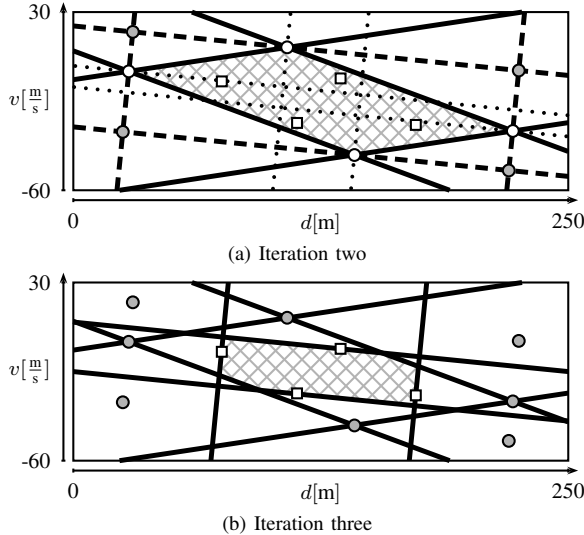


Fig. 6. Iterations two and three of active eMatching

- 2) Perform standard frequency matching for the remaining frequencies.

The situation depicted in Fig. 5 can be used to illustrate the first iteration of the active eMatching, too. During the first iteration of active eMatching, the four matches marked as white circles are identified as eMatches. Now, the unambiguous extreme ( $dv$ )-lines (dashed lines) can be removed from the spectra of the respective ramps. This causes the identification of new extreme frequencies in the modified spectra in iteration two, which is depicted in Fig. 6(a). Note that the unambiguous extreme frequencies from iteration one are removed and four new eMatches (white circles) can be identified. After processing steps 1b) and 1c), the algorithm enters the third iteration given in Fig. 6(b). There, no eMatches can be identified and the algorithm continues with step 2 to find the remaining targets using the standard frequency matching with all frequencies left.

In comparison to passive eMatching, active eMatching may cause additional computations. However, the active eMatching has several significant advantages: Using this algorithm, all matches are found as eMatches for  $M < N$  and obviously this method finds at least as many eMatches as passive eMatching, usually more. In the example discussed in Fig. 5 and 6, active eMatching is able to identify eight targets as eMatches, while passive eMatching only finds four of them.

#### IV. MODULATION DESIGN FOR ACC

The design of the modulation, i.e. the choice of the center frequency  $f_c$  and in particular the frequency ramp slopes  $s_i$  in (3), determines in which regions of the ( $dv$ )-plane extreme matches are more likely to occur. In this section, we design the modulation such that the important targets of the ACC application will be more likely found as eMatches. This approach can be easily adapted to other target distributions and hence applications.

In ACC, targets are roughly distributed as shown in Fig. 7. The distribution was found from real ACC measurements over a distance of about 5000km, mainly on highways. All probability values below  $10^{-5}$  are simply set to zero. In a first attempt, the distribution can be modeled with two modes of a Gaussian mixture model. We distinguish two classes of targets, the moving targets (MT) and the stationary targets (ST). The class ST

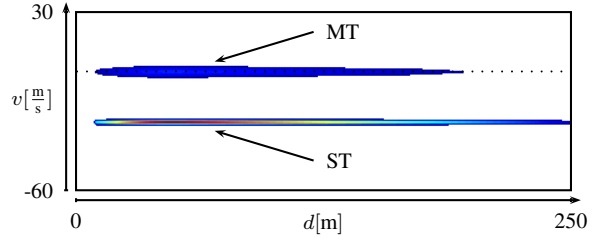


Fig. 7. Target distribution for ACC scenarios

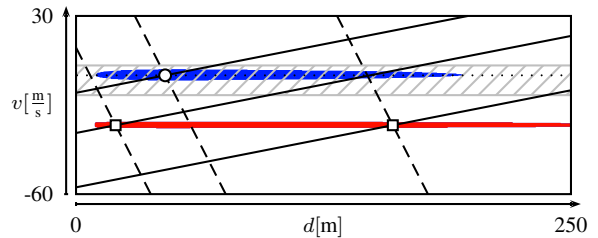


Fig. 8. Modulation design for ACC scenarios

contains fixed objects along the road, e.g. guard rails, traffic signs, and so on. It is characterized by a nearly constant relative velocity of  $v \approx -25.2 \frac{m}{s}$  corresponding to the mean negative velocity of the ego vehicle. All other objects belong to class MT. It is characterized by a relative velocity  $v \approx 0 \frac{m}{s}$ . The mean values  $\mu$ , standard deviations  $\sigma$ , and class probabilities  $P$  of those two classes are given in Table I. To refine the distribution, the target probability was modeled to linearly decay over distance, as targets far away are less likely to be detected. This causes the drop shaped structure of the two modes of the distribution. From the plot of the target distribution, it is already possible to deduce principal design rules for a modulation which is optimized to measure relevant objects in ACC applications as extreme matches. Fig. 8 shows a sketch of the same target distribution as in Fig. 7. The hatched area there shows the region of the ( $dv$ )-plane relevant for ACC, i.e. all targets with a relative velocity  $v \in [-10, 5] \frac{m}{s}$ . The *most relevant object* (MRO) inside that region is often that one with the smallest *time to collision* (equals  $-d/v$ ) among all closing targets. This definition of MRO will also be used for the performance evaluation in section V. A possible location for the MRO in ACC is given by the white circle in Fig. 8. Two white squares indicate the positions of a close and a far stationary target. In addition, ( $dv$ )-lines for all three targets are depicted for a 2-ramp modulation. The first frequency ramp steeply rises (dashed), while the second frequency ramp slowly decays (solid), see Eq. (2). Obviously, in the spectrum of the first ramp (dashed ( $dv$ )-lines), the beat frequency of the relevant ACC-object is between the two beat frequencies caused by the two stationary targets. It is unlikely an extreme frequency. In contrast, the frequency of the ACC-object in the second ramp (solid ( $dv$ )-lines) is likely to be extreme. Hence a modulation for ACC application should contain at least three slowly decaying frequency ramps to identify the relevant ACC objects as eMatches. Slowly rising frequency ramps are a

$\mu_{v,MT}$	$\sigma_{v,MT}$	$P_{MT}$	$\mu_{v,ST}$	$\sigma_{v,ST}$	$P_{ST}$
0 m/s	2 m/s	0.33	-25.2 m/s	0.6 m/s	0.67

TABLE I  
TARGET DISTRIBUTION PARAMETERS IN TYPICAL ACC SCENARIOS

modulation	ramp	slope [MHz/ms]	duration [ms]
A	1	150.0	1.00
	2	-5.0	7.50
	3	-3.0	7.75
	4	-1.0	8.00
B	1,2	$\pm 150.0$	1.00
	3,4	$\pm 75.0$	2.00

TABLE II  
PARAMETERS OF MODULATIONS A AND B

bad choice for ACC application since in this case eMatches will be found for far ACC targets with large distance  $d$ .

### V. SIMULATION RESULTS

In this section, we evaluate the performance of our improved frequency matching algorithms in Monte-Carlo simulations. In each simulation, a large number of real targets is generated according to the ACC target distribution and corresponding beat frequencies are calculated for different modulations. Then we use both passive and active eMatching to determine eMatches and compare them to the real targets. We also study what happens if the ideal assumptions A3-A6 in section III-B are violated in a practical LFMCW radar.

#### A. Modulation parameters

In all simulations, we use two different modulations whose parameters are given in Table II. All ramps are centered at  $f_c = 76.5\text{GHz}$  and a FFT of length 512 is applied to generate the spectra. The part of the  $(dv)$ -plane that can be sensed with the respective modulation is depicted in Fig. 9. The plots show the field of view as the non-hatched region of the  $(dv)$ -plane bounded by the  $(dv)$ -lines for  $|f| = f_{\max}$  on the right-hand side. The lines for  $f = 0\text{Hz}$  on the left-hand side illustrate the slopes of the ramps. Obviously, modulation A fulfills the design rule for ACC from section IV (at least three slowly decaying frequency ramps), while modulation B clearly violates it.

#### B. Simulation setup

In all simulations, the locations of targets are distributed according to the ACC-distribution in Fig. 7. The number of simultaneous targets inside the radar's field of view has also

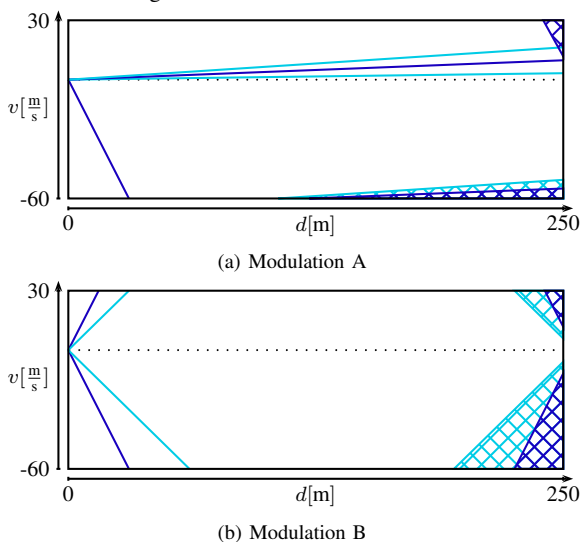


Fig. 9. Field of view of modulation A and B

quantity	description
$P_{\text{target}}$	probability that a real target is found as an eMatch
$P_{\text{mismatch}}$	probability that a mismatch is found as an eMatch
$P_{\text{MRO}}$	probability that the most relevant ACC-object (MRO) is found as an eMatch (refer to section IV)
$(dv)$ -area	statistics calculated for the whole $(dv)$ -plane
ACC-area	statistics calculated for the relevant ACC-area, that contains approx. 33% of the real targets, see Fig. 8

TABLE III  
ALGORITHM PERFORMANCE MEASURES

been found during the measurement mentioned in section IV. It is modeled as a random variable following the *Nakagami* distribution with a shape parameter  $\mu_{\text{Nak}} = 1.54$  and a spread parameter  $\omega_{\text{Nak}} = 144.62$ . This results in a mean number of  $\mu_M = 11.1$  targets with a standard deviation of  $\sigma_M = 4.6$ . In each simulation, a total number of one million targets have been generated. The measures introduced in Table III are used to evaluate the performance of our improved frequency matching.

#### C. Ideal conditions

The first simulation compares the performance of passive and active eMatching under ideal frequency detection conditions, i.e. assumption A3 to A6 from section III-B are all valid. The results are given in Table IV (simulation 1). The first and second line for each modulation shows the results for passive and active eMatching, respectively.

	$(dv)$ -area		ACC-area		
	$P_{\text{target}}$	$P_{\text{mismatch}}$	$P_{\text{target}}$	$P_{\text{mismatch}}$	$P_{\text{MRO}}$
Simulation 1:	Assumption	A3 ✓	A4 ✓	A5 ✓	A6 ✓
A	8.25%	0.00%	11.21%	0.00%	14.16%
	8.57%	0.00%	11.41%	0.00%	14.64%
B	6.93%	0.00%	6.97%	0.00%	12.83%
	7.22%	0.00%	7.20%	0.00%	13.54%
Simulation 2:	Assumption	A3 ✗	A4 ✗	A5 ✓	A6 ✓
A	5.12%	0.00%	6.49%	0.00%	8.70%
	5.25%	0.00%	6.57%	0.00%	8.91%
B	4.78%	0.00%	4.79%	0.00%	8.73%
	4.91%	0.00%	4.90%	0.00%	9.07%
Simulation 3:	Assumption	A3 ✗	A4 ✗	A5 ✗	A6 ✓
A	6.77%	5.41%	8.29%	10.28%	11.04%
	10.13%	11.18%	10.71%	18.40%	14.10%
B	5.18%	0.53%	5.26%	0.59%	9.85%
	6.40%	1.05%	6.12%	0.98%	12.07%
Simulation 4:	Assumption	A3 ✗	A4 ✗	A5 ✗	A6 ✗
A	3.82%	2.17%	0.24%	0.01%	0.83%
	6.06%	6.04%	0.34%	0.03%	1.17%
B	3.15%	0.30%	3.82%	0.29%	4.02%
	3.64%	0.49%	4.25%	0.45%	4.64%

TABLE IV  
SIMULATION RESULTS

As we see, the results for active eMatching are slightly better than those for passive eMatching. No mismatches are labeled as eMatches as expected for these ideal settings. Also note the difference between modulation A and B concerning the ACC-area statistics: While modulation A is able to find the most relevant object for ACC in roughly 14.6% of all cycles for active eMatching, modulation B achieves 13.5%. This confirms our design rule in section IV.

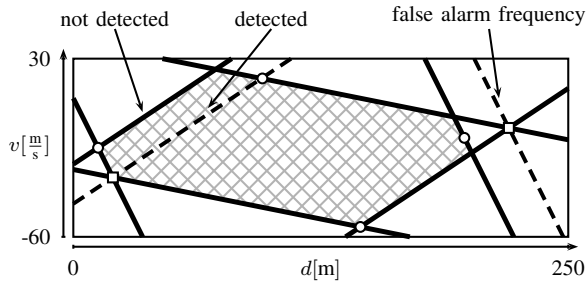


Fig. 10. Mismatches labeled as eMatches due to nonideal detection properties

#### D. Nonideal frequency detection

Now we investigate the consequence of a violation of assumption A3 and A4 from section III-B, i.e. when the frequency detection is not ideal. We assume a probability of spectral detection of  $P_D = 0.9$  and a probability of spectral false alarm of  $P_{FA} = 10^{-3}$ . In both cases,  $P_D < 1$  and  $P_{FA} > 0$ , a wrong frequency might be detected as extreme frequency. As a result, mismatches could be labeled as eMatches. This is illustrated in Fig. 10, where the true extreme ( $dv$ )-lines caused by a modulation with three ramps and four targets (white circles) are plotted bold. Due to nonideal frequency detection, two mismatches (white squares) are found as eMatches. The wrong eMatch on the left-hand side arises because a real extreme frequency is not detected. Hence the frequency next to it (plotted dashed) is considered to be extreme. The eMatch on the right-hand side is a mismatch, too, because a false alarm frequency (plotted dashed) outside the hatched region is detected.

The results of this simulation are given in Table IV (simulation 2). The first observation is that the values for  $P_{\text{target}}$  and  $P_{\text{MRO}}$  have decreased to roughly 63% compared to simulation 1. This is not surprising as we have  $P_D^N = 0.9^4 \approx 65.6\%$ . At a first glance, one might expect a decrease to  $0.9^3 = 72.9\%$ , as three extreme ( $dv$ )-lines are sufficient to form an eMatch. But note that besides the three extreme frequencies needed to form an eMatch, the frequencies in the remaining ramps still have to be detected to form a match. The reason that there are still no mismatches ( $P_{\text{mismatch}} = 0$ ) is that assumption A5 is still valid. This means, there is no error in frequency estimation and hence the algorithm searches for perfect intersections of  $N$  ( $dv$ )-lines only. At the position of a real target, the ( $dv$ )-lines do intersect perfectly. But to form a mismatch, a perfect intersection of all  $N$  ( $dv$ )-lines at a position where no real target resides is necessary. Although this is not impossible, the probability for this event to happen is zero for a Monte-Carlo simulation.

In simulation 3 of Table IV, we added an error to the estimated beat frequency, modeled by a zero-mean Gaussian random variable with a standard deviation of  $\frac{1}{3}$  FFT-bin. As expected, the values for  $P_{\text{mismatch}}$  are increased, as approximate intersections have to be accounted for now, leading to mismatches being labeled as eMatches. Obviously, modulation A is more susceptible to label mismatches as eMatches under these nonideal detection properties. We also observe that active eMatching performs worse than passive eMatching regarding the mismatch probability  $P_{\text{mismatch}}$ .

#### E. Missing IQ-mixer

In the last experiment, we study the violation of assumption A6, i.e. if the LFM CW radar is not equipped with an IQ-mixer. Then the sign of the beat frequency is unknown, posing a serious

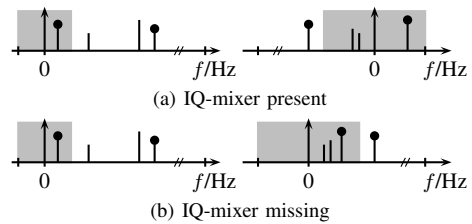


Fig. 11. Classification of extreme frequencies

problem in the detection of extreme frequencies. In Fig. 11(a), two spectra of an upswing and a downswing ramp are plotted with four target beat frequencies. An IQ-mixer is supposed to be present. The extreme frequencies are marked with a dot. Fig. 11(b) illustrates the same situation if no IQ-mixer is present. Then all spectra are symmetric and it is sufficient to show the positive frequencies only. Obviously, in the spectrum of the right ramp, one of the former extreme frequencies will not be detected as extreme frequency anymore. The gray area marks that part of a spectrum, where the order of beat frequencies can change without an IQ-mixer. If such a change occurs, a wrong frequency is considered to be extreme and mismatches might be labeled as an eMatch.

Simulation results for a missing IQ-mixer and nonideal frequency detection are given in Table IV (simulation 4). Over the whole ( $dv$ )-plane, the fraction of matches found as eMatches decreased in comparison to simulation 3. More interesting are the results in the ACC region for modulation A. There, almost no eMatches occur without an IQ-mixer. The reason becomes clear if we take the field of view of modulation A into account, refer to Fig. 9(a) again. A target inside the ACC region is close to the zero frequency in the three downswing ramps. Due to the symmetry of the spectra without an IQ-mixer, the frequencies of ACC targets are very unlikely to be extreme frequencies now. In other words, a missing IQ-mixer will significantly degrade the performance of eMatching for ACC targets.

## VI. CONCLUSION

We have presented a framework to extend the standard frequency matching in LFM CW radar by exploiting extreme frequencies. It reliably classifies matches as targets or mismatches under certain conditions. We have studied the existence of extreme matches, developed two improved frequency matching algorithms, and formulated some basic rules for the modulation design in ACC applications. We also presented simulation results of our improved frequency matching algorithms.

## ACKNOWLEDGMENT

This research has been conducted in cooperation with the Robert Bosch Corporation, to which the authors would like to express their gratitude.

## REFERENCES

- [1] N. Levanon and E. Mozeson, *Radar Signals*, 1st ed. Hoboken, New Jersey: John Wiley & Sons, 2004.
- [2] L. Lovász and M. Plummer, *Matching Theory*, 1st ed. Budapest: Akadémiai Kiadó, 1986.
- [3] U. Luebbert, "Target Position Estimation with a Continuous Wave Radar Network," Ph.D. dissertation, Technische Universität Hamburg-Harburg, 2005.
- [4] A. Rényi, "On Projections of Probability Distributions," *Acta Mathematica Hungarica*, vol. 3, no. 3, pp. 131–142, 1952.
- [5] M. Schoor and B. Yang, "High-Resolution Angle Estimation for an Automotive FMCW Radar Sensor," in *International Radar Symposium*, Cologne, Sep. 2007.